Molecular Crystals and Liquid Crystals

Publication details, including instructions for authors and subscription information:
http://www.tandfonline.com/loi/gmcl20

# Two Dimensionally Ion-Conductive Liquid Crystals of Cholesterol/Tetra(Ethylene Oxide) Block Molecules

Kenji Kishimoto [a], Yoshimitsu Sagara [a], Takashi Kato [a], Tomohiro Mukai [b], Hiroyuki Ohno [b] & Nobuyuki Tamaoki [c]

[a] Department of Chemistry and Biotechnology, School of Engineering, The University of Tokyo, Hongo, Bunkyo-ku, Tokyo, Japan

[b] Department of Biotechnology, Tokyo University of Agriculture and Technology, Koganei, Tokyo, Japan

[c] National Institute of Advanced Industrial Science and Technology (AIST), Higashi, Tsukuba, Ibaraki, Japan

Version of record first published: 31 Aug 2006

*Mol. Cryst. Liq. Cryst.*, Vol. 435, pp. 117/[777]–125/[785], 2005

ISSN: 1542-1406 print/1563-5287 online
DOI: 10.1080/15421400590954623

Taylor & Francis
Taylor & Francis Group



# Two Dimensionally Ion-Conductive Liquid Crystals of Cholesterol/Tetra(Ethylene Oxide) Block Molecules

**Kenji Kishimoto**
**Yoshimitsu Sagara**
**Takashi Kato**
Department of Chemistry and Biotechnology, School of Engineering, The University of Tokyo, Hongo, Bunkyo-ku, Tokyo, Japan

**Tomohiro Mukai**
**Hiroyuki Ohno**
Department of Biotechnology, Tokyo University of Agriculture and Technology, Koganei, Tokyo, Japan

**Nobuyuki Tamaoki**
National Institute of Advanced Industrial Science and Technology (AIST), Higashi, Tsukuba, Ibaraki, Japan

*Two-dimensionally ion-conductive liquid crystals have been simply obtained by self-assembly of a cholesterol/tetra(ethylene oxide) block molecule and lithium triflate. Nanophase-segregation between cholesterol and tetra(ethylene oxide) blocks leads to the formation of a smectic A liquid crystalline phase in a wide range of temperature. A homeotropically aligned lithium salt complex in the smectic A phase shows two-dimensional ionic conductivity. The ionic conductivities parallel to the smectic layers are higher than those perpendicular to the layers. The maximum value of the anisotropy in the ionic conductivity is about* $2.4 \times 10^3$ *at* $30^\circ C$.

**Keywords:** anisotropic ion-conduction; liquid crystals; macroscopic orientation; nanophase-segregation

Financial support of Grant-in-Aid for Scientific Research on Priority Areas, Scientific Research B, Encouragement of Young Scientists B (No. 15350077) from the Ministry of Education, Culture, Sports, Science, and Technology is gratefully acknowledged. K. K. is thankful for financial support by the Research Fellowships of the Japan Society for the Promotion of Science (JSPS) for Young Scientists.

Address correspondence to Takashi Kato, Department of Chemistry and Biotechnology, School of Engineering, The University of Tokyo, Hongo, Bunkyo-ku, Tokyo, 113-8656, Japan. E-mail: kato@chiral.t.u-tokyo.ac.jp

## INTRODUCTION

Anisotropic nanostructures of liquid crystals can be used for the fabrication of new functional materials [1–5]. For example, low-dimensional ion-active materials have been developed [6–8]. However, no molecular orientation was achieved and anisotropic ionic conductivities could not be measured before we recently prepared low-dimensional ion-conductive materials based on poly(ethylene oxide)s (PEOs) [3,9–12] and ionic liquids [13–16]. For these materials, we could achieve molecular alignment and the measurements of anisotropic ionic conductivities. These anisotropic ion-conductors are mainly composed of two incompatible blocks: an ion-conductive moiety such as poly(ethylene oxide)s or ionic liquids and an ion-insulating mesogenic moiety.

Columnar and layered assemblies are formed for these materials due to nanophase-segregation of these blocks. Monodomain of these anisotropic nanophase-segregated structures is effective for low-dimensional ion conduction. To obtain such highly oriented liquid crystalline (LC) structures, the design of mesogenic core is important. For PEO-based anisotropic ion-conductors, calamitic mesogens having several aromatic rings are often used to induce smectic LC phases [9–12]. A wide temperature range of smectic A phase is favorable for the monodomain formation. However, the aromatic molecules tend to show complicated transition behavior of the ordered smectic phases, which are difficult to form monodomains.

In this study, we have designed and synthesized two types of block PEO-based liquid crystals with cholesteryl groups as the mesogenic cores. Cholesterol can induce smectic A phases for various types of molecules, while it is known to act as a chiral nematogen [17–22]. We here show that cholesterol/tetra(ethylene oxide) block molecules and their complexes with lithium salts show stable smectic A phases in wide ranges of temperature.

## RESULTS AND DISCUSSION

The preparation of block liquid crystals **1** and **2** has been achieved in only one synthetic reaction through a coupling of cholesterylchloroformate and tetraethylene glycol.

### Liquid Crystalline Properties

The liquid crystalline properties of **1** and **2** have been examined with a polarized optical microscope, a differential scanning calorimetry, and

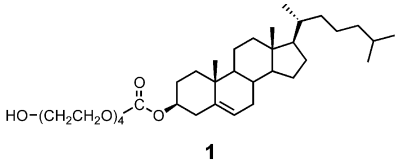


**1**

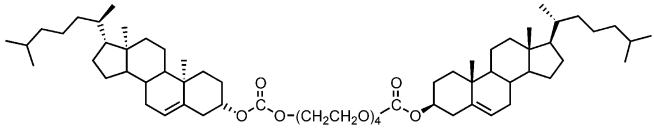


**2**

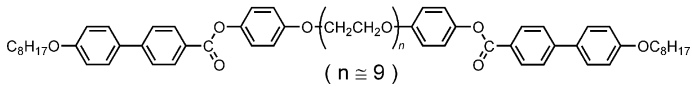


**3**

**CHART 1**

an X-ray diffractometer. Table 1 summarizes the liquid crystalline behavior of the block liquid crystals. Compounds **1** and **2** show enantiotropic smectic A phases in wide ranges of temperature including room temperature. In contrast, block liquid crystal **3** with dimeric calamitic mesogens and its lithium salt complex exhibit narrower temperature ranges of smectic A phases [9] than cholesterol block liquid crystals. They tend to show ordered smectic phases in the lower temperature.

**TABLE 1** Phase Transition Behavior of PEO-Based Block Liquid Crystals and their Lithium Salt Complexes

| | Phase transition behavior[a] | | | | | | | | | | |
|---|---|---|---|---|---|---|---|---|---|---|---|
| **1** | | | | | | | G | −35 | $S_A$ | 103 | Iso |
| **1**/$LiOSO_2CF_3$[b] | | | | | | | G | −26 | $S_A$ | 130 | Iso |
| **2** | | | | | | | G | 13 | $S_A$ | 107 | Iso |
| **2**/$LiOSO_2CF_3$[b] | | | | | | | G | 19 | $S_A$ | 114 | Iso |
| **3**[c] | G | −46 | $S_X$ | 57 | $S_E$ | 77 | $S_B$ | 121 | $S_A$ | 170 | Iso |
| **3**/$LiOSO_2CF_3$[b,c] | G | −28 | $S_X$ | 48 | $S_E$ | 73 | $S_B$ | 121 | $S_A$ | 178 | Iso |

[a]Transition temperature (°C): Iso = isotropic, $S_A$ = smectic A, $S_B$ = smectic B, $S_E$ = smectic E, $S_X$ = unidentified ordered smectic phases, G = glassy.

[b]The concentration of lithium salts is 0.05 mol per oxyethylene unit.

[c]Ref. [9].

Lithium triflate ($LiOSO_2CF_3$) is added to **1** and **2** as an ionic species. The concentration of lithium is 0.05 mol per ethylene oxide unit. The incorporation of lithium salts increases the transition temperatures (Table 1). The ion–dipole interaction between lithium ions and the oxygens of oligoether induces the formation and stabilization of the nanophase-segregated layered structures.

Figure 1 shows the polarized optical micrographs of the lithium salt complex of **1** (**1**/$LiOSO_2CF_3$) at room temperature. This complex easily forms homeotropic alignment on the substrates (glass and indium-tin-oxide (ITO)) when it is cooled from the isotropic phase. On the other hand, the lithium salt complex of dimeric block liquid crystals (**2**/$LiOSO_2CF_3$) forms polydomains on the substrates. The volume balance between cholesterol blocks and tetra(ethylene oxide) blocks is also important for molecular orientation. In this case, the increase of hydrophobic cholesterol block may destabilize the monodomain formation on the hydrophilic surface of the substrates.

X-ray diffraction pattern of **1**/$LiOSO_2CF_3$ shows that the layer spacing of the smectic A phase is 5.7 nm at room temperature. On the other hand, the extended conformation of compound **1** is calculated to be 3.3 nm with a molecular modeling. These results indicate that the lithium salt complex of **1** forms a nanophase-segregated bilayer structure and effective ion-conductive paths are formed for the oriented complex (Fig. 2).

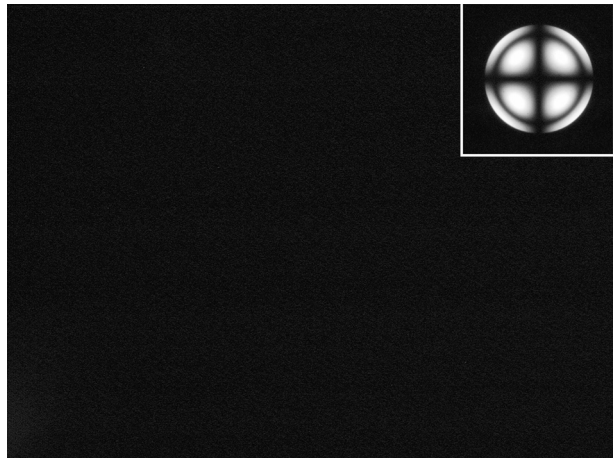

**FIGURE 1** Polarized optical micrograph of **1**/$LiOSO_2CF_3$ at room temperature. Inset shows the conoscopic image of the complex.

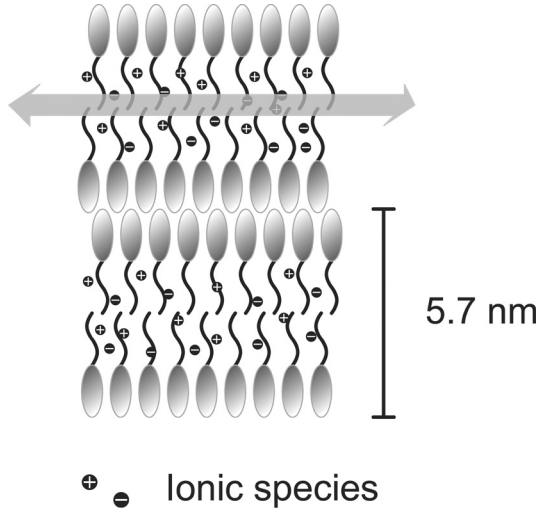


**FIGURE 2** Schematic illustration of bilayer nanostructures of **1**/$LiOSO_2CF_3$.

## Anisotropic Ionic Conductivity

The anisotropic ionic conductivities of **1**/$LiOSO_2CF_3$ have been measured by the complex impedance methods. The lithium salt complex is filled within two types of cells as schematically illustrated in Figure 3. Cell A is comb-shaped gold electrodes shaded on a glass substrate and cell B is a pair of ITO substrates. The complex

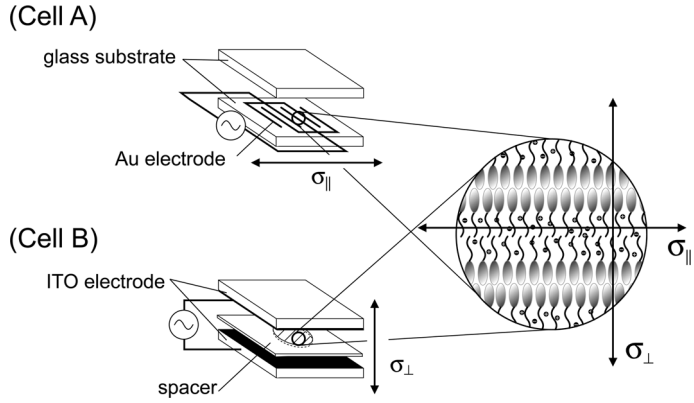


**FIGURE 3** Schematic illustration of comb-shaped gold electrodes (Cell A) and ITO electrodes (Cell B) used for the measurements of anisotropic ionic conductivities.

spontaneously forms homeotropic alignment on both types of cells, which has been confirmed by conoscopic observation with a polarized optical microscope. This macroscopic orientation of **1**/$LiOSO_2CF_3$ allows us to measure the anisotropic ionic conductivities. The ionic conductivities parallel ($\sigma_{\parallel}$) and perpendicular ($\sigma_{\perp}$) to the smectic layers can be obtained by using cell A and cell B, respectively.

Figure 4 shows the Arrhenius plots of ionic conductivities of **1**/$LiOSO_2CF_3$ as a function of temperature. The values of $\sigma_{\parallel}$ (●) are higher than those of $\sigma_{\perp}$ (○) in the smectic A phase. For example, the $\sigma_{\parallel}$ and $\sigma_{\perp}$ values at 30°C are $5.0 \times 10^{-6}$ and $2.1 \times 10^{-9}$ S cm$^{-1}$, respectively. The magnitude of anisotropy in the ionic conductivity ($\sigma_{\parallel}/\sigma_{\perp}$) is about $2.4 \times 10^3$ at the same temperature. The anisotropy of the ionic conductivity disappears when the complex turns into the isotropic phase. It should be noted that $\sigma_{\perp}$ values are successfully measured for **1**/$LiOSO_2CF_3$. The $\sigma_{\perp}$ values of **3**/$LiOSO_2CF_3$ could not be

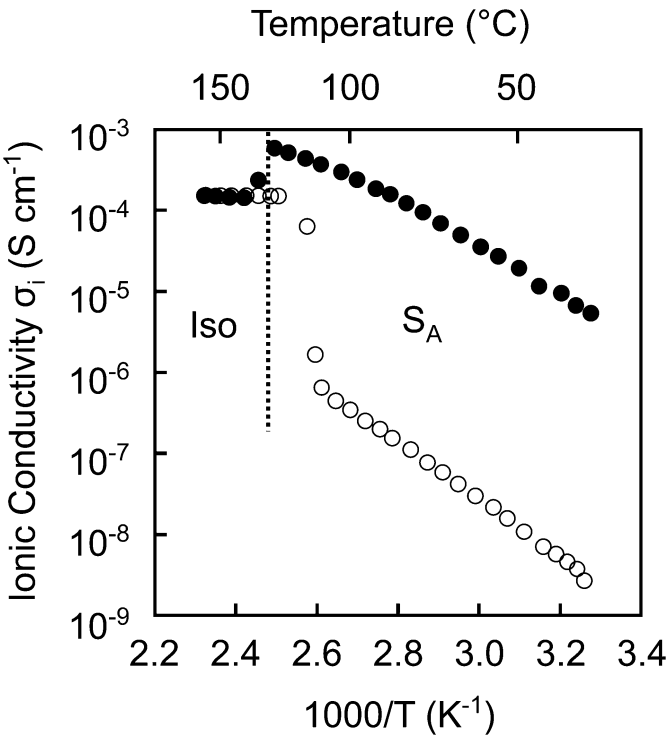


**FIGURE 4** Arrhenius plots of anisotropic ionic conductivities of **1**/$LiOSO_2CF_3$. Filled (●) and open (○) circles represent the ionic conductivities parallel ($\sigma_{\parallel}$) and perpendicular ($\sigma_{\perp}$) direction to the smectic layers, respectively.

obtained because they did not form homeotropic alignment on ITO substrates. [9] Moreover, the $\sigma_{\parallel}$ values of **1**/$LiOSO_2CF_3$ are higher than those of **3**/$LiOSO_2CF_3$. The value of $\sigma_{\parallel}$ at 30°C was $8.8 \times 10^{-7}$ S cm$^{-1}$ for **3**/$LiOSO_2CF_3$. Monodomain structures in the smectic A phase may contribute to the relatively higher ionic conductivities for **1**/$LiOSO_2CF_3$. Cholesterol/tetra(ethylene oxide) block molecule **1** has advantages for the fabrication of two-dimensional anisotropic ion-conductors based on the stable smectic A phase.



## CONCLUSION

Cholesterol/tetra(ethylene oxide) block liquid crystals have been prepared by one-step synthesis. The lithium salt complexes of the block liquid crystals exhibit the smectic A phases in wide ranges of temperature including room temperature. Two-dimensionally anisotropic ion-conductive behavior can be achieved for the highly oriented lithium salt complexes of **1**. These two-dimensionally anisotropic ion-conductors have potentials for a new type of ion-active devices such as polyelectrolytes, ion-transporting membranes, or ion-sensors.

## EXPERIMENTAL

### Characterization

Liquid-crystalline phases and molecular orientation were determined with an Olympus BH-2 polarized optical microscope equipped with a Mettler FP82HT hot-stage. Phase transition temperatures were detected by a NETZSCH DSC 204 Phoenix differential scanning calorimeter. Heating and cooling rates were 10°C/min. The transition temperatures were taken at the maximum of exothermic and minimum point of endothermic peaks, respectively. The midpoint of the change in the heat capacity was taken as a glass transition temperature. X-ray diffraction study in the present study was conducted on a Rigaku RINT-2500 system using CuK$\alpha$ radiation. Molecular modeling was calculated with a software CS Chem3DPro employing MM2 energy minimization parameters.

### Synthesis

#### *2-(2-(2-(2-(cholesteryloxycarbonyloxy)ethoxy)ethoxy) ethoxy)ethanol (1)*

Tetraethylene glycol (6.98 g, 36.0 mmol) and pyridine (10 mL) were dissolved in dry dichloromethane ($CH_2Cl_2$) (30 mL). A $CH_2Cl_2$ solution

of cholesterylchloroformate (2.94 g, 6.55 mmol) was added slowly dropwise to the mixture at 0°C with stirring, and the solution was stirred for an additional 24 h at room temperature. The resultant mixtures were poured into water and extracted with chloroform three times with a separate funnel. The combined organic phases were washed with saturated $NH_4Cl$ aqueous solution and brine. The organic phase was dried over magnesium sulfate, filtered through a Celite pad, and concentrated under reduced pressure. The crude product was purified by column chromatography (eluent: hexane/ethyl acetate = 1/2) to give **1** (3.24 g, 5.33 mmol) as a smectic liquid crystal at room temperature in a yield of 82%.

$^1$H NMR (400 MHz, $CDCl_3$): $\delta$ = 0.68–2.03 (m, 42H), 2.37–2.40 (m, 2H), 3.61–3.75 (m, 14H), 4.28 (t, $J$ = 9.3 Hz, 2H), 5.39–5.40 (m, 1H).

$^{13}$C NMR (100 MHz, $CDCl_3$): $\delta$ = 11.8, 18.7, 19.3, 21.0, 22.6, 22.8, 23.8, 24.3, 27.7, 28.0, 28.2, 31.8, 31.9, 35.8, 36.2, 36.5, 36.8, 38.0, 39.5, 39.7, 42.3, 50.0, 56.1, 56.7, 61.8, 66.6, 69.0, 70.3, 70.5, 70.6, 70.7, 72.5, 77.9, 122.9, 139.3, 154.5.

### *Bis(cholesteryloxycarbonyl)tetraethylene Glycol (2)*

Quantities: tetraethylene glycol ($1.54 \times 10^{-1}$ g, $7.93 \times 10^{-f1}$ mmol); cholesteryl chloroformate ($9.94\,10^{-1}$ g, 2.21 mmol). The experimental procedure of **2** was the same as described for the preparation of compound **1**. The crude product was purified by column chromatography (eluent: hexane/ethyl acetate = 3/1) to give **2** ($7.49 \times 10^{-1}$ g, $7.34 \times 10^{-1}$ mmol) as a white solid in a yield of 93%.

$^1$H NMR (400 MHz, $CDCl_3$): $\delta$ = 0.67–2.02 (m, 84H), 2.36–2.42 (m, 4H), 3.61–3.75 (m, 12H), 4.28 (t, $J$ = 4.8 Hz, 4H), 5.39–5.40 (m, 2H).

$^{13}$C NMR (100 MHz, $CDCl_3$): $\delta$ = 11.8, 18.7, 19.2, 21.0, 22.5, 22.8, 23.8, 24.3, 27.6, 28.0, 28.2, 31.8, 31.9, 35.8, 36.2, 36.5, 38.0, 39.5, 39.7, 42.3, 50.0, 56.1, 56.7, 66.7, 68.9, 70.6, 77.9, 122.9, 139.3, 154.5.

## Preparation of Lithium Salt Complexes

To obtain lithium salt complexes, cholesterol/tetra(ethylene oxide) block liquid crystals and lithium triflate were dissolved in dry tetrahydrofuran followed by drying in vacuo at room temperature for 24 h.

## Measurements of Ionic Conductivity

Dynamic anisotropic ionic conductivities were examined by using an impedance analyzer (Schlumberger, Solartron 1260) with a custom set-up temperature controller.

## REFERENCES


[1] Kato, T. (2002). *Science*, *295*, 2414.
[2] Kato, T. & Mizoshita, N. (2002). *Curr. Opin. Solid State Mater. Sci.*, *6*, 579.
[3] Kishimoto, K., Yoshio, M., Mukai, T., Yoshizawa, M., Ohno, H., & Kato, T. (2003). *J. Am. Chem. Soc.*, *125*, 3196.
[4] van Nostrum, C. F. & Nolte, R. J. M. (1996). *Chem. Commun.*, 2385.
[5] Percec, V., Glodde, M., Bera, T. K., Miura, Y., Shiyanovskaya, I., Singer, K. D., Balagurusamy, V. S. K., Heiney, P. A., Schnell, I., Rapp, A., Spiess, H.-W., Hudson, S. D., & Duan, H. (2002). *Nature*, *419*, 384.
[6] Hubbard, H. V. St. A., Sills, S. A., Davies, G. R., McIntyre, J. E., & Ward, I. M. (1998). *Electrochim. Acta.*, *43*, 1239.
[7] Dias, F. B., Batty, S. V., Ungar, G., Voss, J. P., & Wright, P. V. (1996). *J. Chem. Soc.*, *Faraday Trans.*, *92*, 2599.
[8] Imrie, C. T., Ingram, M. D., & McHattie, G. S. (1999). *Adv. Mater.*, *11*, 832.
[9] Ohtake, T., Ogasawara, M., Ito-Akita, K., Nishina, N., Ujiie, S., Ohno, H., & Kato, T. (2000). *Chem. Mater.*, *12*, 782.
[10] Ohtake, T., Takamitsu, Y., Ito-Akita, K., Kanie, K., Yoshizawa, M., Mukai, T., Ohno, H., & Kato, T. (2000). *Macromolecules*, *33*, 8109.
[11] Ohtake, T., Ito, K., Nishina, N., Kihara, H., Ohno, H., & Kato, T. (1999). *Polym. J.*, *31*, 1155.
[12] Ohtake, T., Kanie, K., Yoshizawa, M., Mukai, T., Ito-Akita, K., Ohno, H. & Kato, T. (2001). *Mol. Cryst. Liq. Cryst.*, *364*, 589.
[13] Yoshio, M., Mukai, T., Ohno, H., & Kato, T. (2004). *J. Am. Chem. Soc.*, *126*, 994.
[14] Yoshio, M., Mukai, T., Kanie, K., Yoshizawa, M., Ohno, H., & Kato, T. (2002). *Adv. Mater.*, *14*, 351.
[15] Yoshio, M., Mukai, T., Kanie, K., Yoshizawa, M., Ohno, H., & Kato, T. (2002). *Chem. Lett.*, 320.
[16] Hoshino, K., Yoshio, M., Mukai, T., Kishimoto, K., Ohno, H., & Kato, T. (2003). *J. Polym. Sci. Part A: Polym. Chem.*, *41*, 3486.
[17] Tamaoki, N., Aoki, Y., Moriyama, M., & Kidowaki, M. (2003). *Chem. Mater.*, *15*, 719.
[18] Mallia, V. A. & Tamaoki, N. (2004). *Chem. Soc. Rev.*, *33*, 76.
[19] Tamaoki, N. (2001). *Adv. Mater.*, *13*, 1135.
[20] Rabatic, B. M., Pralle, M. U., Tew, G. N., & Stupp, S. I. (2003). *Chem. Mater.*, *15*, 1249.
[21] Harwood, S. M., Toyne, K. J., Goodby, J. W., Parsley, M., & Gray, G. W. (2000). *Liq. Cryst.*, *27*, 443.
[22] Vora, R. A. & Teckchandani, V. R. (1991). *Mol. Cryst. Liq. Cryst.*, *209*, 285.